





A Decision Support System For Early Stage Parkinson's Diagnosis from EEG Data Using Symbolic Mutual Information and KAC Features

Neslihan Baki^{1*} , Nurhan Gürsel Özmen² 

¹ Karadeniz Technical University, Health Sciences Institute, Department of Medical Informatics and Biostatistics, Trabzon, Türkiye, neslihanbaki520@gmail.com

² Karadeniz Technical University, Faculty of Engineering, Department of Mechanical Engineering, Trabzon, Türkiye, gnurhan@ktu.edu.tr

*Corresponding Author

ARTICLE INFO

ABSTRACT

Keywords:
Parkinson
Electroencephalography
Weighted Symbolic Mutual Information (wSMI)
Kolmogorov Algorithmic Complexity (KAC)
Extreme gradient boosting algorithm

Parkinson's disease (PD) is a serious neurological disease that is threatening the whole world population. The devolution of the neurons located in the substantia nigra of the brain causes, bradykinesia, rigidity and resting tremor, which are characteristic motor symptoms, occurring in advanced stages. Currently, there is not an effective treatment for PD, it is just controlled by some prescriptions. Early detection of this disease affects the choice of treatment. Recent studies on early diagnosis by analyzing electroencephalography (EEG) recordings have provided a glimmer of hope. Therefore, in this study, an efficient PD detection method from EEG data by using a new set of features is searched. An opensource resting state data of 28 subjects divided as Parkinson and control groups were analyzed. PSDs of the EEG frequency bands that are delta, theta, alpha, beta and gamma and Median Spectral Frequency (MSF), Spectral Entropy (SE), Kolmogorov Algorithmic Complexity (KAC) and Weighted Symbolic Mutual Information (wSMI) were extracted as features. The performance of the PD and control group was evaluated with Gradient Boosting (GB), Gaussian Naive Bayes (GNB), and K-nearest Neighbor (KNN), Support Vector Machines (SVM), Logistic Regression (LR), Categorical Boosting (CatBoost) and Extreme Gradient Boosting (XGBoost) Algorithms. A 85% accuracy was achieved with the XGBoost algorithm, using 31 channels and 13 features which outperforms the results of previous studies using this dataset in the literature.

Article History:

Received: 28.09.2023

Accepted: 26.08.2024

Online Available: 14.10.2024

1. Introduction

Parkinson's disease (PD) is a progressive, neuronal degeneration disorder that is caused by genetic and environmental factors and affects considerable amount of people all around the world [1]. Many research were done on the symptoms, causes, and the treatments of PD till now [2]. Various motor and non-motor symptoms due to damage of nigrostriatal dopaminergic nerve cells and other nerve cells are observed. Basic motor symptoms include bradykinesia, rigidity, postural instability, tremor

and non-motor symptoms include cognitive, behavioral, sleep, and autonomic disorders [3-6].

It is often difficult to diagnose PD in its primer stage. A neurologist generally makes the diagnosis based on a clinical examination of the patient and an assessment of the patient's medical history. Since the symptoms are not specific to the disease, there may be misdiagnosis or delays [7]. These delays impose enormous costs on both the people and the health systems of countries. Early diagnosis of the disease affects the choice of treatment. Initiation of neuroprotective treatment to protect the nerves before too much

loss of nerve cells in the substantia nigra may slow the progression of PD.

In recent years, electroencephalography (EEG) recordings are being used for diagnosing PD [8-10]. Since a clear temporal resolution of the cortical electrical activity of EEG is achieved, it is mostly preferred for clinical and research use. Moreover, it is cheaper and easy to use, compared to MEG.

Recent EEG studies on PD, showed that the amplitudes of theta and alpha brain waves change significantly with the slowing actions [10]. In order to reveal the hidden information about the differences during PD needs more attention to implement new methods in the analysis of EEG. These studies may also contribute to the discovery of other functions and dysfunctions of the brain. It is stated that if there is any deformation in the substantia nigra neurons, it will affect the information transfer between the cortex and the basal ganglia. These changes can also be revealed from EEG recordings [11, 12]. During PD, the EEG spectrum slows down [13, 14]. Based on these changes, classification of PD and healthy control (HC) groups can be detected. Moreover, decision support systems can be developed.

Research on PD diagnosis from EEG data mostly focus on the development of new signal processing methods for feature extraction [15]. Linear features acquired from different frequency bands have achieved around 75-82% accuracy [16] whereas, nonlinear methods have also been used to extract information from EEG for PD diagnosis [17, 18] where around 80-95% classification accuracy rates were calculated. Besides feature extraction methods, the use of different machine learning methods and comparison of their performances are also searched [19].

Chaturvedi et al. compared high-resolution EEG measurements of 50 PD patients and 41 HC and found that the theta power in the left temporal region and the alpha1/theta ratio in the mid left region were the most effective variables in classification. Among machine learning methods, 56%, 78%, 74% and 68% accuracy

results were obtained with Logistic Regression (LR), Random Forest, Support Vector Machines (SVM) and Decision Tree, respectively [20]. Betrouni et al. achieved 84% and 88% classification accuracy using Power Spectral Density (PSD) features with SVM and K-nearest Neighbor Algorithm (KNN) methods in classifying the level of cognitive impairment in PD [21]. Anjum et al. achieved 85.7% accuracy in their classification with a linear predictive coding for PD detection from EEG [22].

Loh et al. transformed EEG data into spectrograms to train a two-dimensional convolutional neural network model by applying Gabor transform to resting state EEG data from 16 individuals with HC and 15 individuals with PD, achieving 99.46% classification accuracy [23]. Lee et al. proposed a prediction method with 89.3% accuracy in classification using Hjorth parameter features and Gradient Boosting (GB) algorithm [24]. Suuronen et al. investigated how the number and placement of electrodes affect PD and HC subjects. Using a special budget-based search algorithm to select optimized channel sets for classification, they achieved an accuracy of 76% [25]. Karakaş et al. achieved 85.7% accuracy in the Iova data and 63.25% accuracy in the Turku data sets using beta activity and amplitude reduction in EEG signals associated with PD [26].

Onay et al. used triaxial accelerometer signals collected during a pedaling task in 13 HC, 13 PD and 13 FoG symptomatic individuals, the perceptual latency from the movement command to the start of the movement was estimated for each session. Features of the distributions of the latencies of each participant were extracted and 69.2% success was achieved with SVM [27]. Orkan Olcay et al. used entropy and connectivity properties of chemosensor-derived EEG signals together to discriminate PD and HC with odor stimuli with over 80% classification performance [28].

Moreover, some deep learning studies in the literature have achieved higher classification results [29, 30]. The main drawback is that, they require high processing time and large data. On the other hand, a successful classification

performance can be achieved by using classical machine learning methods due to the limited data size.

Most of the studies in the literature analyze EEG data of whole channels. Fewer studies searched for the regional and number of electrodes based differences. In this study, the data of 63 channels and 31 channels were analyzed by excluding Pz as it is the reference channel. The 31 channels analyzed in this study consist of Fp1, AF3, F7, F3, FC1, FC5, T7, C3, CP1, O1, Oz, O2, CP5, P3, P7, PO3, PO4, P4, P8, CP6, CP2, C4, T8, FC6, FC2, F4, F8, AF4, Fp2, Fz, Cz.

This study proposes novel features to extract prominent features of EEG signals that can be used as biomarkers to identify Parkinson's patients with the help of machine learning algorithms. In this study, wSMI, KAC and SE features were used for the first time in PD classification in resting state EEG data. The classical and new established ensemble learning algorithms are used to diagnose PD. GB, Gaussian Naive Bayes (GNB), KNN, SVM, LR, Categorical Boosting Algorithm (CatBoost) and, Extreme Gradient Boosting Algorithm (XGBoost) are used with different metrics.

In classification studies for PD diagnosis based on EEG, generally the accuracy metric is included. In these studies, 69.77% of the data used consisted of balanced classes, and the remaining percentage did not show a balanced distribution. Training data with unbalanced classes can lead to prediction errors and poor generalizations. In studies with patients, especially for the diagnosis of a disease, sensitivity, specificity, and accuracy measures are very useful in evaluating the results of the model, as they provide a measure of true positives. In this study, classification results were evaluated according to Accuracy, Precision, Recall, F1 score and AUC. The average number of electrodes in studies in the literature is 43.34 ± 62.18 [19, 31].

The next section of the study continues with the "Material - Method" section, where data sets and signal processing methods are introduced. In this section, the features and classifiers are briefly described. In the third section, the results

obtained using different classifiers are presented comparatively for different performance measures. Related discussions are summarized here. The last section summarizes the conclusions of the study.

2. Materials and Methods

2.1. Methods

The open-source EEG dataset from the Narayanan Laboratory at the University of Iowa is used [32]. The dataset contains resting state EEG recordings of 14 PD and 14 HC groups. The EEG recordings were done by using Brain Vision 64-channel electrodes system placed on the head according to the international 10-20 system. The HC group was recruited from physically and mentally healthy subjects who were demographically matched with PD in terms of gender and age and had no history of neuropsychiatric disorders. All of the participants signed the written informed consent form. In Table 1, demographic information of the dataset is given. EEG recordings contains 2 minutes eyes open data with 500 Hz sampling frequency and a sampling rate of 0.1-100 Hz. The 64 channels 10-20 EEG electrode locations are shown in Figure 1. The Pz channel was selected as the reference channel.

Table 1. Iowa dataset demographic information for PD and HC groups

Status	PD and HC groups	
	<i>PD</i>	<i>HC</i>
Number	14	14
Gender (male/female)	8f/6m	8f/6m
Age (mean years \pm SD)	70.5 ± 8.7	70.5 ± 8.7
NAART	–	–
MMSE	–	–
MOCA	25.9 ± 2.7	27.2 ± 1.7
UPDRS	13.4 ± 6.6	–
PD years of	5.6 ± 3.2	–

The mean PSD changes of 28 subjects and 31 channels are given in Figure 2.

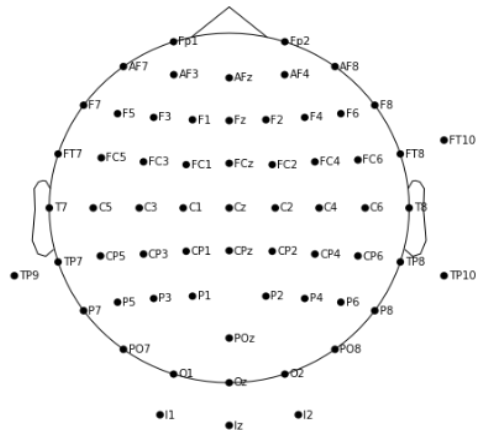


Figure 1. EEG 10-20 Electrode Placement System for 64 channels

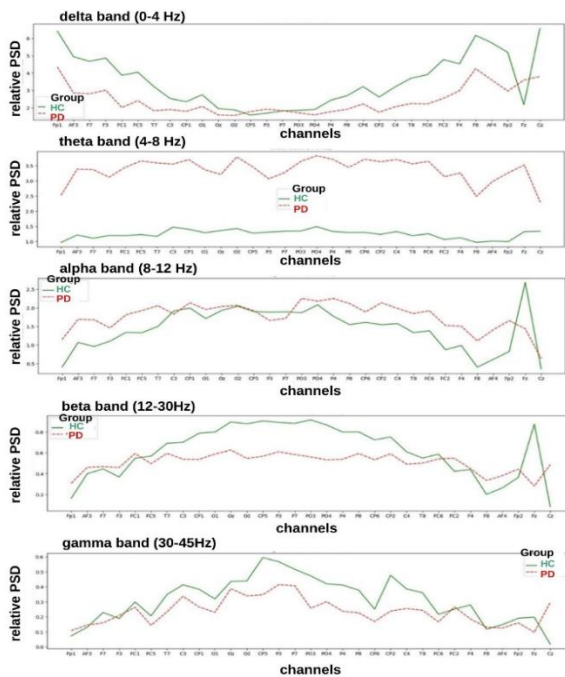


Figure 2. PD and HC relative PSD of 28 contacts and 31 channel frequency bands

In Figure 2, delta, theta, alpha, beta, and gamma frequency bands are given per channel. There is a clear difference both between PD and HC groups, that is, they have different relative PSD values. A reduction of beta rhythm in frontal and central regions, and another reduction of gamma rhythm in central, parietal, and temporal regions was observed, rather than the Fp2, AF3 channels.

In Figures 3-4, EEG topographic maps of PD and HC groups are given. Most of them are in gamma and beta bands, and slightly in alpha, more activation is observed in the HC group compared to PD. These differences are in accordance with the existing literature [1, 8-9].

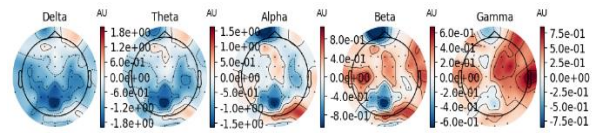


Figure 3. Topographic maps of band power in five frequency bands of the HC group

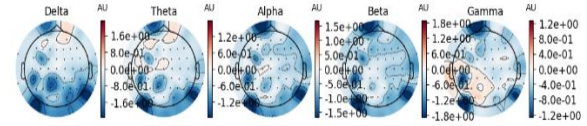


Figure 4. Topographic maps of band power in five frequency bands of the PD group

2.2. Preprocessing

All stages of data analysis were performed with Python using CPU in the Google Colab environment. In order to process EEG data with Python, many libraries such as mne, numpy, pandas, matplotlib, etc. were installed and configured in the Google Colab Python environment.

Since EEG data was recorded in the Brain Vision System, raw EEG files with vhdr extension were transferred to the Google Colab environment by converting them into raw objects with the mne library so that they can be processed in Python language. The data was transferred from other libraries. The data was first bandpass filtered between 0.5 Hz low and 45 Hz high frequencies and notch filtered at 60 Hz and 100 Hz. After filtering, these signals were divided into a non-overlapping time window length of twenty seconds. Then, MSF, PSD theta, wSMI theta, wSMI beta features were extracted and binary classification was performed using CatBoost, XGBoost, GNB, KNN, SVM, GB and LR algorithms. In Figure 5, data analysis steps are depicted.

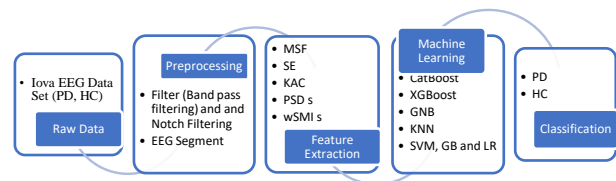


Figure 5. EEG data analysis scheme

2.3. Feature extraction

Feature extraction is the transformation of the unprocessed data into digital values with a reduced size of dimension to lessen the complexity of processing information in which, the original signal characteristics are correctly decoded and evaluated with a well-performing classifier [33]. There are various studies that used PSD parameters from the subbands of decomposed EEG signals which obtained successful classification results [22]. In this study, the PSD of the five bands of the EEG signal, wSMI Delta, wSMI Theta, wSMI alpha, wSMI Beta, wSMI Gama and MSF, SE, KAC, are selected as the feature vector.

2.3.1. Power spectral density

PSD is the measure of the power content of a signal with respect to frequency. It allows time-varying signals to be transferred to the frequency domain, resulting in power distributions of the frequency ranges of the signal [34]. The power distribution of a random signal at different frequencies is calculated by Fourier transform. The PSD equation is given in equation (1).

$$S(f) = \int_{-\infty}^{\infty} R(t)e^{-2\pi if} dt = F(R(t)) \quad (1)$$

2.3.2. Calculation of weighted symbolic mutual information

The Weighted Symbolic Mutual Information (wSMI) measure is increasingly applied to EEG [35, 36]. It is based on the interactions between two signals and the non-linear coupling between them. In a selected tau time k samples of the signal are selected. The magnitudes of the samples are defined by a set of symbols based on the order relation which represents the temporal separation of the signals. In this data set, wSMI is calculated for the joint probability of each pair of symbols. In order to decrease the false correlations between two signal groups, the joint probability matrix P, is multiplied by binary weights. The wSMI can be calculated with the statement in equation (2), where X, and Y represent two different signals.

$$wSMI(X, Y) = \frac{1}{\log k!} \sum_{x \in X} \sum_{y \in Y} w(x, y) p(x, y) \log \left(\frac{p(x, y)}{p(x)p(y)} \right) \quad (2)$$

2.3.3. Median spectral frequency

The Median Spectral Frequency (MSF) is commonly used to show spectral change. It represents the midpoint of the power distribution of the compressed EEG spectral array. It is a measure of the frequency above and below 50% of the total power in the EEG. MSF is also defined as half of the total power [37]. The definition of MSF is given in equation (3):

$$\sum_{j=1}^{MDF} P_j = \sum_{j=MDF}^M P_j = 1/2 \sum_{j=1}^M P_j \quad (3)$$

2.3.4. Spectral entropy

Spectral Entropy is the spectral power distribution of a signal based on Shannon entropy [38]. It indicates the flatness or complexity of the signal spectrum [39]. In the following, SE is calculated by equation (4).

$$H(x, fs) = - \sum_{f=0}^{fs/2} P(f) \log_2 [P(f)] \quad (4)$$

Where P is the normalized PSD and fs is the sampling frequency.

2.3.5. Kolmogorov algorithmic complexity

The Algorithmic Complexity or Kolmogorov complexity (KAC) is related to the minimum description length. The KAC of a sequence s is the length of the shortest run that computes s. It expresses the concepts of simplicity and complexity. If the length d(s) of an array s with the fewest bits is the minimum, this is the minimum description of s. Here d(s) is the Kolmogorov complexity of s and is represented by K(s) [40]. It is represented by equation (5).

$$K(s) = |d(s)| \quad (5)$$

2.4. Classification

The EEG dataset contains a total of 28 data sets belonging to 14 PD and 14 HC groups. 10-fold cross-validation is used for classification. With this technique, the total data set is divided into k approximately equal parts. Machine learning structures are trained and tested k times. Each time, the part of the data to be tested is taken from the k chunks and all the remaining data is used for training the machine learning structure. The

PSD features of five frequency bands (MSF, KAC, wSMI Delta, wSMI Theta and wSMI Alpha) are selected and the performance of different classifiers on PD and HC group data is evaluated using Accuracy, Precision, F1 score, Recall, ROC-AUC metrics. Binary classification was performed with CatBoost, XGBoost, GNB, KNN, SVM, LR and GB algorithms in Python Google Colab environment.

2.4.1. Gradient boosting algorithm

GB algorithm is a method in which new models are created that account for the error in the previous model and then the residuals are added to make the final prediction. It creates prediction models similar to decision trees (Random Forests) for regression and classification problems. The GB algorithm does not create nodes after each tree to make an improvement. Instead, it starts with a leaf. This leaf represents an initial estimate for all weights. The first estimate here is the average value. Then Gradient Boost creates a tree. Boosting differs from other classification algorithms in that it often compensates for the lack of weak learners [41]. GB algorithms can be customized according to the needs of the application, such as learning according to different loss functions. When used for classification, Log-Loss is used as the cost function.

2.4.2. K Nearest neighbor algorithm

KNN is a well-known supervised learning algorithm commonly preferred in classification. This algorithm searches for the closest points to the new point. K is the number of nearest neighbors of the unknown point which is usually chosen as an odd number. In the K-NN method, the output is the class membership. An object is attained to the selected label by a majority vote of its neighbors [42].

2.4.3. Gaussian naive bayes classifier

Naive Bayes Classification, is a simplified version of Bayes' theorem with the independence premise. Bayes' theorem is expressed in equation (6); normal distribution of features

$$P(A|B) = \frac{P(B|A)P(A)}{P(B)} \quad (6)$$

$P(A|B)$ denotes the probability of event A when event B occurs, $P(B|A)$ denotes the probability of event B when event A occurs. $P(A)$ and $P(B)$ show the a priori probabilities of events A and B, adding subjectivity to Bayes' theorem [43]. Naive Bayes classifiers perform well especially with a small set of training data to estimate the necessary parameters.

2.4.4. Support vector machines

SVM is a supervised learning method with three main components that are statistical learning theory, optimization algorithm and kernel functions [44]. In SVM, the most appropriate line separation is the one with equal and maximum distance to the data classes. While creating this maximum distance, called the margin, the samples that are closest to the separating line among the samples belonging to the data classes are used. These examples are called support vectors. In multidimensional space, lines are replaced by hyperplanes [45].

2.4.5. Logistic regression

LR, binary logistic model or logit model is a statistical approach that models the probability of a problem occurring between two alternatives by taking the logarithm of the rates for a problem. In this method, mathematical modeling is performed in order to define the relationship between independent variables and two or multi-class categorical dependent variables [46]. When all independent variables are continuous, the logistic model is calculated with an expression given in equation (7);

$$\ln \frac{\Pr(x_1, \dots, x_p)}{1 - \Pr(x_1, \dots, x_p)} = \beta_0 + \sum_{j=1}^k \beta_j x_{ij} \quad (7)$$

2.4.6. Categorical boosting algorithm

CatBoost is a new ensemble learning method derived from the GB and Decision Tree algorithms proposed by Yandex and shown to have the ability to deal well with heterogeneous data [47]. Moreover, CatBoost uses balanced forgetful trees as base predictors. Thus, it

overcomes the problems of overlearning. In general, it exhibits superior classification performance compared to other ensemble learning algorithms.

2.4.7. Extreme gradient boost algorithm

XGBoost is a high performance version of the GB algorithm that is optimized with various adjustments. It is quick, has high predictive power, can avoid overlearning, can manage empty data. The first step in XGBoost, is to make the first prediction. The prediction can be any number as it will converge with the operations to be performed in the next steps and the correct result will be reached. The first tree is completed by constructing the trees that predict the errors, calculating the similarity and gain scores for the trees, pruning and obtaining the model outputs [48].

3. Results and Discussion

For all machine learning algorithms used in this study, k-layer cross-validation was used to evaluate the overall accuracy, as it provides much better and more reliable results than conventional training methods (e.g. 75% training data, 25% test data) [49]. Based on the classical and newly used features, PSD of five frequency bands, SE, MSF, KAC, wSMI Delta, wSMI Theta, wSMI Alpha, wSMI Beta, wSMI Gamma the performance of different classifiers on the PD and HC group data was evaluated using Accuracy, Precision, F1 score, Recall, ROC-AUC metrics. The classification results are shown in Table 2 and Table 3 respectively, analyzing 63 channels and 31 channels.

Table 2. 10-fold cross-validation results of 63 channels

Classifier	Accuracy	Precision	Recall	F1 Score
XGBoost	0.63 (+/- 0.16)	0.45 (+/- 0.25)	0.57 (+/- 0.19)	0.48 (+/- 0.21)
CatBoost	0.83 (+/- 0.16)	0.70 (+/- 0.31)	0.77 (+/- 0.23)	0.72 (+/- 0.28)
GNB	0.58 (+/- 0.32)	0.50 (+/- 0.37)	0.57 (+/- 0.33)	0.51 (+/- 0.35)
KNN	0.51 (+/- 0.21)	0.36 (+/- 0.26)	0.52 (+/- 0.20)	0.40 (+/- 0.23)
GB	0.63 (+/- 0.22)	0.47 (+/- 0.29)	0.57 (+/- 0.25)	0.50 (+/- 0.27)
SVM	0.56 (+/- 0.30)	0.52 (+/- 0.34)	0.57 (+/- 0.31)	0.51 (+/- 0.32)
LR	0.46 (+/- 0.26)	0.42 (+/- 0.33)	0.52 (+/- 0.28)	0.42 (+/- 0.28)

Table 3. 10-fold cross-validation results of 31 channels

Classifier	Accuracy	Precision	Recall	F1 Score
XGBoost	0.85 (+/- 0.18)	0.85 (+/- 0.22)	0.87 (+/- 0.16)	0.83 (+/- 0.24)
CatBoost	0.81 (+/- 0.18)	0.78 (+/- 0.26)	0.82 (+/- 0.19)	0.77 (+/- 0.22)
GNB	0.75 (+/- 0.27)	0.68 (+/- 0.34)	0.72 (+/- 0.30)	0.69 (+/- 0.32)
KNN	0.58 (+/- 0.29)	0.48 (+/- 0.34)	0.57 (+/- 0.29)	0.49 (+/- 0.31)
GB	0.68 (+/- 0.18)	0.57 (+/- 0.28)	0.65 (+/- 0.22)	0.57 (+/- 0.25)
SVM	0.66 (+/- 0.25)	0.58 (+/- 0.33)	0.65 (+/- 0.27)	0.58 (+/- 0.30)
LR	0.46 (+/- 0.26)	0.41 (+/- 0.33)	0.55 (+/- 0.26)	0.42 (+/- 0.28)

The XGBoost algorithm achieved the highest accuracy among the seven classifiers. The confusion matrixes and ROC-AUC results of the classifiers are shown in Figure 6 and Figure 7. XGBoost correctly predicted 12 and incorrectly predicted 2 of the 14 HC groups and correctly predicted 12 and incorrectly predicted 2 of the 14 PD groups as given in Figure 6. The second best performing classifier is the CatBoost classifier, with 12 correct and 2 incorrect predictions of the 14 HC groups. Whereas, 11 correct and 3 incorrect predictions of the 14 PD groups. The amount of True Positives and True Negatives is decreasing with GNB, KNN, SVM, GB and LR algorithms, respectively.

The ROC curves and AUC values are seen in Figure 7. It is observed from the figure that, the XGBoost has the best separation capability for the proposed features. However, SVM, LR and GB have lower AUC values. Although they use the same feature sets, the best separation methodologies of the Machine Learning Algorithms bring this difference.

The present study has 13 features, belonging to PSD of five frequency bands, and SE, MSF, KAC, wSMI Delta, wSMI Theta, wSMI Alpha, SMI Beta, wSMI Gamma. A successful classification accuracy was achieved compared to the machine learning results in the literature.

The wSMI feature, KAC and SE features in this study were used for the first time in detecting PD from the resting state EEG data. The study in [50], is expanded with channel reduction and cross-validation parameters.

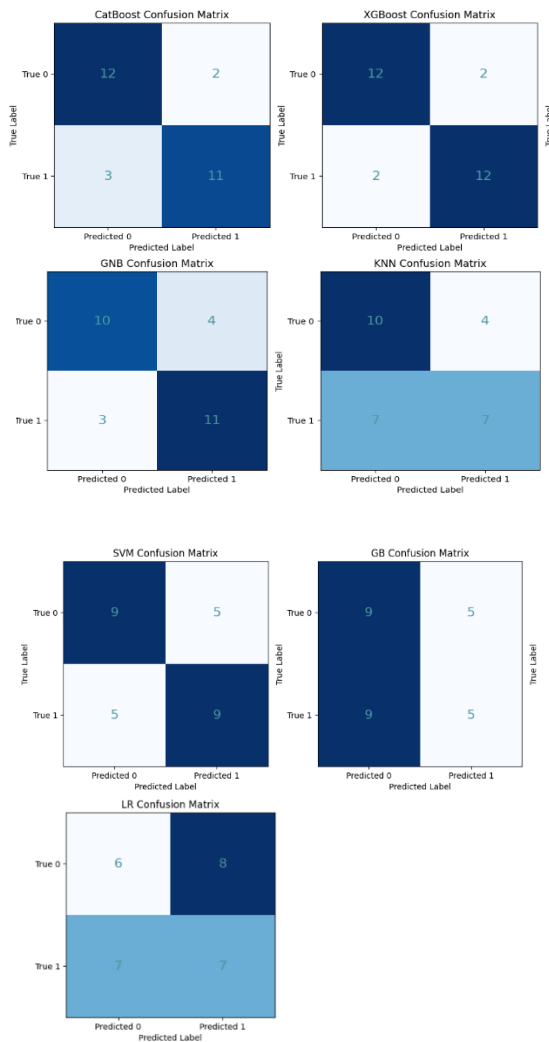


Figure 6. Confusion matrixes of classifiers

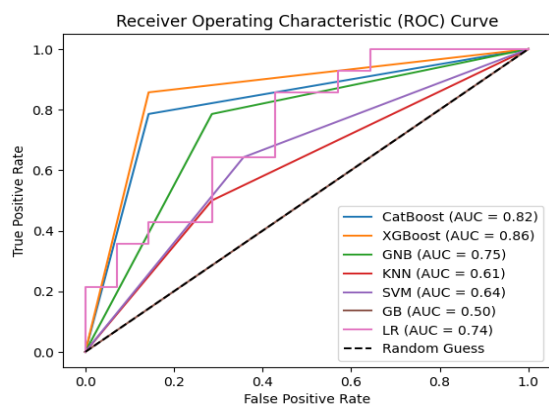


Figure 7. ROC curve and AUC values for classifiers

In the literature, accuracy metric is generally used in PD detection studies from EEG [19, 31]. In this study, precision, sensitivity, F1 score, AUC metrics were used. It is seen that the results are supporting each other. Resting EEG or magnetoencephalogram (MEG) activity in PD patients undergoes a general loss of complexity compared to controls [51, 52]. The KAC features

used in this paper are in accordance with that result. Studies have shown that beta and gamma band power is decreased in PD [53, 54]. Abnormalities in the beta band have been shown to be associated with dyskinesia (involuntary movements) in PD [55]. Therefore, the use of band power features are consistent with this view. New feature sets and channel-based studies will be continued to examine degeneration in different regions of the brain for future work.

4. Conclusion

In this study, new features wSMI, KAC, SE, MSF and subband PSDs were extracted from 63 channels and 31 channels of EEG data. They were analyzed by several machine learning algorithms for two different set of channels. According to the results, the 31 channel accuracies and AUC performances are higher than the 63 channels with all algorithms. The use of fewer channels reduces the processing time for online applications. A successful classification accuracy (85.00%) and 0.86 AUC value were obtained with XGB algorithm. Compared to the literature, a successful classification result was obtained. The use of novel features yielded a successful classification that can be a tool for PD diagnosis.

Article Information Form

Funding

The author (s) has no received any financial support for the research, authorship or publication of this study.

Authors' Contribution

The authors contributed equally to the study.

The Declaration of Conflict of Interest/ Common Interest

No conflict of interest or common interest has been declared by the authors.

The Declaration of Ethics Committee Approval

This study does not require ethics committee permission or any special permission.

The Declaration of Research and Publication Ethics

The authors of the paper declare that they comply with the scientific, ethical and quotation rules of SAUJS in all processes of the paper and that they do not make any falsification on the data collected. In addition, they declare that Sakarya University Journal of Science and its editorial board have no responsibility for any ethical violations that may be encountered, and that this study has not been evaluated in any academic publication environment other than Sakarya University Journal of Science.

Copyright Statement

Authors own the copyright of their work published in the journal and their work is published under the CC BY-NC 4.0 license.

References

- [1] J. Valls-Sole, F. Valdeoriola, "Neurophysiological correlate of clinical signs in parkinson's disease," *Clinical Neurophysiology*, vol. 113, no. 6, pp. 792–805, 2002.
- [2] J. Parkinson, "An essay on the shaking palsy," *The Journal of Neuropsychiatry and Clinical Neurosciences*, vol. 14, no. 2, pp. 223–236, 2002.
- [3] I. G. McKeith, D. Galasko, K. Kosaka, E. K. Perry, D. W. Dickson, L. A. Hansen, D.P. Salmon, J. Lowe, S.S. Mirra, E.J. Byrne, G. Lennox, N.P. Quinn, J.A. Edwardson, P.G. Ince, C. Bergeron, A. Burns, B.L. Miller, S. Lovestone, D. Collerton, E.N.H. Jansen, C. Ballard, R.A.I. de Vos, G.K. Wilcock, K.A. Jellinger, R.H. Perry, "Consensus guidelines for the clinical and pathologic diagnosis of dementia with Lewy bodies (DLB)," *Neurology*, vol. 47, no. 5, pp. 1113–1124, 1996.
- [4] J. Q. Trojanowski, "Neurodegeneration: The Molecular Pathology of Dementia and Movement Disorders," in D.W. Dickson (Ed.), ISN Press, Basel, 2003, pp. 11-13.
- [5] J. Jankovic, "Pathophysiology and assessment of parkinsonian symptoms and signs," in *Handbook of Parkinson's Disease*, 3rd ed., R. Pahwa, K. Lyons, and W.C. Koller, Eds. Taylor and Francis Group, LLC, New York, pp. 79-104, 2007.
- [6] C. H. Waters, "Diagnosis and Treatment of Parkinson's Disease," translated by B. Büyükkal, Turgut Publishing and Trade Co. Ltd., Istanbul, 2000.
- [7] H. Braak, K. Del Tredici, H. Bratzke, J. Hamm-Clement, D. Sandmann-Keil, U. Rüb "Staging of the intracerebral inclusion body pathology associated with idiopathic parkinson's disease (preclinical and clinical stages)," *Journal of Neurology*, vol. 249, no. 0, pp. 1–1, 2002.
- [8] C. Pappalettera, F. Miraglia, M. Cotelli, P. M. Rossini, F. Vecchio, "Analysis of complexity in the EEG activity of parkinson's disease patients by means of approximate entropy," *GeroScience*, vol. 44, no. 3, pp. 1599–1607, 2022.
- [9] D. Stoffers, J. L. W. Bosboom, J. B. Deijen, E. C. Wolters, H. W. Berendse, C. J. Stam, "Slowing of oscillatory brain activity is a stable characteristic of parkinson's disease without dementia," *Brain*, vol. 130, no. 7, pp. 1847–1860, 2007.
- [10] S. Kan, K. Satoshi, M. Akihiko, H. Motohiko, M. Tomohiko, Y. Hirokazu, Y. Mai, T. Jun, H. Kaname, "Comparison of quantitative EEGs between parkinson disease and age-adjusted normal controls," *Journal of Clinical Neurophysiology*, vol. 25, no. 6, pp. 361–366, 2008.
- [11] N. Fogelson, D. Williams, M. Tijssen, G. van Bruggen, H. Speelman, P. Brown, "Different functional loops between cerebral cortex and the subthalamic area in parkinson's disease," *Cerebral Cortex*, vol. 16, no. 1, pp. 64–75, 2006.
- [12] E. Lalo, S. Thobois, A. Sharott, G. Polo, P. Mertens, A. Pogosyan, P. Brown, "Patterns of bidirectional communication between cortex and basal ganglia during movement in patients with parkinson disease," *The*

- Journal of Neuroscience, vol. 28, no. 12, pp. 3008–3016, 2008.
- [13] J. L. W. Bosboom, D. Stoffers, C.J. Stam, B.W. van Dijk, J. Verbunt, H.W. Berendse, E.Ch. Wolters, “Resting state oscillatory brain dynamics in parkinson’s disease: An MEG study,” *Clinical Neurophysiology*, vol. 117, no. 11, pp. 2521–2531, 2006.
- [14] H. Tanaka, T. Koenig, R. D. Pascual-Marqui, K. Hirata, K. Kochi, D. Lehmann, “Event-related potential and EEG measures in parkinson’s disease without and with dementia,” *Dementia and Geriatric Cognitive Disorders*, vol. 11, no. 1, pp. 39–45, 2000.
- [15] R. Yuvaraj, P. Thagavel J. Thomas, J. Fogarty, F. Ali, “Comprehensive Analysis of Feature Extraction Methods for Emotion Recognition from Multichannel EEG Recordings,” *Sensors*. 23(2):915, vol. 23, no. 2, pp. 915, 2023.
- [16] G. Liu, Y. Zhang, Z. Hu, X. Du, W. Wu, C. Xu, X. Wang, S. Li, “Complexity analysis of electroencephalogram dynamics in patients with parkinson’s disease,” *Parkinson’s Disease*, vol. 2017, pp. 1–9, 2017.
- [17] T. M. McKenna, T. A. McMullen, M. F. Shlesinger, “The brain as a dynamic physical system,” *Neuroscience*, vol. 60, no. 3, pp. 587–605, 1994.
- [18] C. Lainscsek, M. E. Hernandez, J. Weyhenmeyer, T. J. Sejnowski, H. Poizner, “Non-linear dynamical analysis of EEG time series distinguishes patients with parkinson’s disease from healthy individuals,” *Frontiers in Neurology*, vol. 4, 2013.
- [19] A. M. Maitin, A. J. García-Tejedor, J. P. Munoz, “Machine learning approaches for detecting parkinson’s disease from EEG Analysis: A systematic review,” *Applied Sciences*, vol. 10, no. 23, p. 8662, 2020.
- [20] M. Chaturvedi, F. Hatz, U. Gschwandtner, J. G. Bogaarts, A. Meyer, P. Fuhr, V. Roth, “Quantitative eeg (QEEG) measures differentiate parkinson’s disease (PD) patients from healthy controls (HC),” *Frontiers in Aging Neuroscience*, vol. 9, Jan. 2017.
- [21] N. Betrouni, A. Delval, L. Chaton, L. Defebvre, A. Duits, A. Moonen, A. F. G. Leentjen, K. Dujardin, “Electroencephalography-based machine learning for cognitive profiling in parkinson’s disease: Preliminary results,” *Movement Disorders*, vol. 34, no. 2, pp. 210–217, Oct. 2018.
- [22] Md F. Anjum, S. Dasgupta, R. Mudumbai, A. Singh, J. F. Cavanagh, N. S. Narayanan, “Linear predictive coding distinguishes spectral EEG features of parkinson’s disease,” *Parkinsonism and amp; Related Disorders*, vol. 79, pp. 79–85, Oct. 2020.
- [23] H. W. Loh, C. P. Ooi, E. Palmer, P. D. Barua, S. Dogan, T. Tuncer, M. Baygin, U. R. Acharya, “GaborPDNet: Gabor Transformation and Deep Neural Network for parkinson’s disease detection using EEG signals,” *Electronics*, vol. 10, no. 14, p. 1740, Jul. 2021.
- [24] S. B. Lee, Y. J. Kim, S. Hwang, H. Son, S. K. Lee, K. I. Park, Y. G. Kim, “Predicting parkinson’s disease using gradient boosting decision tree models with Electroencephalography signals,” *Parkinsonism and amp; Related Disorders*, vol. 95, pp. 77–85, Feb. 2022.
- [25] I. Suuronen, A. Airola, T. Pahikkala, M. Murtojarvi, V. Kaasinen, H. Railo, “Budget-based classification of parkinson’s disease from resting state EEG,” *IEEE Journal of Biomedical and Health Informatics*, vol. 27, no. 8, pp. 3740–3747, Aug. 2023.
- [26] M. F. Karakaş, F. Latifoğlu, “Distinguishing parkinson’s disease with GLCM features from the Hankelization of

- EEG Signals,” *Diagnostics*, vol. 13, no. 10, p. 1769, May 2023.
- [27] F. Onay, B. Karaçalı, “Accelerometer-based timing analysis for parkinson’s disease classification,” 2023 31st Signal Processing and Communications Applications Conference (SIU), Jul. 2023.
- [28] B. O. Olcay, F. Onay, G. Akın Öztürk, A. Öviz, M. Özgören, T. Hummel, Ç. Güdücü “Using chemosensory-induced EEG signals to identify patients with de Novo Parkinson’s disease,” *Biomedical Signal Processing and Control*, vol. 87, p. 105438, Jan. 2024.
- [29] S. L. Oh, Y. Hagiwara, U. Raghavendra, R. Yuvaraj, N. Arunkumar, M. Murugappan, U. Rajendra Acharya, “A deep learning approach for parkinson’s disease diagnosis from EEG signals,” *Neural Computing and Applications*, vol. 32, no. 15, pp. 10927–10933, 2018.
- [30] L. Qiu, J. Li, J. Pan, “Parkinson’s disease detection based on multi-pattern analysis and multi-scale convolutional Neural Networks,” *Frontiers in Neuroscience*, vol. 16, 2022.
- [31] A. M. Maitin, J. P. Romero Munoz, A. J. Garcia-Tejedor, “Survey of machine learning techniques in the analysis of EEG signals for parkinson’s disease: A systematic review,” *Applied Sciences*, vol. 12, no. 14, p. 6967, 2022.
- [32] “Narayanan lab,” Datasets | Narayanan Lab, <https://narayanan.lab.uiowa.edu/article/datasets> (accessed Sep. 18, 2023).
- [33] S. Krishnan, Y. Athavale, “Trends in biomedical signal feature extraction,” *Biomedical Signal Processing and Control*, vol. 43, pp. 41–63, 2018.
- [34] “Power_spectral_density,” Wikipedia, https://en.wikipedia.org/wiki/Spectral_density#Power_spectral_density (accessed Sep. 18, 2023).
- [35] J. R. King, J. D. Sitt, F. Faugeras, L. Cohen, L. Naccache, L. Cohen, L. Naccache, S. Dehaene, “Information sharing in the brain indexes consciousness in noncommunicative patients,” *Current Biology*, vol. 23, no. 19, pp. 1914–1919, 2013.
- [36] J. D. Sitt, J. R. King, I. E. Karoui, B. Rohaut, F. Faugeras, A. Gramfort, L. Cohen, M. Sigman, S. Dehaene, L. Naccache, “Large scale screening of neural signatures of consciousness in patients in a vegetative or minimally conscious state,” *Brain*, vol. 137, no. 8, pp. 2258–2270, 2014.
- [37] A. Phinyomark, P. Phukpattaranont, C. Limsakul, “Feature reduction and selection for EMG Signal Classification,” *Expert Systems with Applications*, vol. 39, no. 8, pp. 7420–7431, 2012.
- [38] H. Helakari, J. Kananen, N. Huotari, L. Raitamaa, T. Tuovinen, V. Borchardt, A. Rasila, V. Raatikainen, T. Starck, T. Hautaniemi, T. Myllyla, O. Tervonen, S. Rytky, T. Keinanen, V. Korhonen, V. Kiviniemi, H. Ansakorpi, “Spectral entropy indicates electrophysiological and hemodynamic changes in drug-resistant epilepsy a multimodal MREG study,” *NeuroImage: Clinical*, vol. 22, p. 101763, 2019.
- [39] A. Vakkuri, A. Yli Hankala, P. Talja, S. Mustola, H. Tolvanen-Laakso, T. Sampson, H. Viertiö-Oja, “Time-frequency balanced spectral entropy as a measure of anesthetic drug effect in central nervous system during sevoflurane, propofol, and thiopental anesthesia,” *Acta Anaesthesiologica Scandinavica*, vol. 48, no. 2, pp. 145–153, Jan. 2004.
- [40] “Kolmogorov_complexity,” Wikipedia, https://en.wikipedia.org/wiki/Kolmogorov_complexity (accessed Sep. 18, 2023).
- [41] A. Natekin, A. Knoll, “Gradient Boosting Machines, a tutorial,” *Frontiers in Neurorobotics*, vol. 7, 2013.

- [42] “K-nearest neighbors algorithm,” Wikipedia, https://en.wikipedia.org/wiki/K-nearest_neighbors_algorithm (accessed Sep. 18, 2023).
- [43] “Naive Bayes Classifier,” Wikipedia, https://tr.wikipedia.org/wiki/Naive_Bayes_s%C4%B1n%C4%B1fland%C4%B1r%C4%B1c%C4%B1s%C4%B1 (accessed Sep. 18, 2023).
- [44] V. N. Vapnik, *The Nature of Statistical Learning Theory*. Cham: Springer International Publishing.
- [45] C. J. C. Burges, “Data Mining and Knowledge Discovery,” vol. 2, no. 2, pp. 121–167, 1998.
- [46] W. Menard, Scott. *Logistic regression: From introductory to advanced concepts and applications*. Sage, 2010.
- [47] L. Prokhorenkova, G. Gusev, A. Vorobev, A. V. Dorogush, A. Gulin, “CatBoost: unbiased boosting with categorical features.” *Advances in neural information processing systems* 31, 2018.
- [48] V. Morde, “XGBoost algorithm: Long may she reign!” *Medium*, <https://towardsdatascience.com/https-medium-com-vishalmorde-xgboost-algorithm-long-she-may-rein-edd9f99be63d> (accessed May 26, 2024).
- [49] E. Alpaydin. *Introduction to machine learning*. MIT press, 2020.
- [50] N. Baki, N. Gürsel Özmen, “An early diagnosis approach for parkinson patients without cognitive disorder from EEG Data,” 2022 Medical Technologies Congress (TIPTEKNO), Antalya, Turkey, 2022, pp. 1-4, doi: 10.1109/TIPTEKNO56568.2022.996020. Oct. 2022.
- [51] C. Gomez, K. T. E. Olde Dubbelink, C. J. Stam, D. Abasolo, H. W. Berendse, R. Hornero, “Complexity analysis of resting-state MEG activity in early-stage parkinson’s disease patients,” *Annals of Biomedical Engineering*, vol. 39, no. 12, pp. 2935–2944, 2011.
- [52] G. S. Yi, J. Wang, B. Deng, X. L. Wei, “Complexity of resting-state EEG activity in the patients with early-stage Parkinson’s disease,” *Cognitive Neurodynamics*, vol. 11, pp. 147-160, 2017.
- [53] L. Pezard, R. Jech, E. Ruzicka, “Investigation of non-linear properties of multichannel EEG in the early stages of Parkinson’s disease,” *Clinical Neurophysiology*, vol. 165, no. 1, pp. 38–45, 2001, PMID: 11137659.
- [54] J. Bosboom, D. Stoffers, C. Stam, B. Dijk, J. Verbunt, H. Berendse, E.Ch. Wolters, “Resting state oscillatory brain dynamics in Parkinson’s disease: An MEG study,” *Clinical Neurophysiology*, vol. 117, no. 11, pp. 2521–2531, 2006.
- [55] Q. Wang, L. Meng, J. Pang, X. Zhu, D. Ming, “Characterization of EEG data revealing relationships with cognitive and motor symptoms in Parkinson's disease: A systematic review,” *Frontiers in Aging Neuroscience*, cilt 12, sayı 587396, 2020.